A review on applications of Cu_2ZnSnS_4 as alternative counter electrodes in dye-sensitized solar cells

Anurag Roy, Parukuttaymma Sujatha Devi, Smagul Karazhanov, D. Mamedov, Tapas Kumar Mallick, and Senthilarasu Sundaram

Citation: AIP Advances **8**, 070701 (2018); doi: 10.1063/1.5038854
View online: https://doi.org/10.1063/1.5038854
View Table of Contents: http://aip.scitation.org/toc/adv/8/7
Published by the American Institute of Physics

A review on applications of Cu_2ZnSnS_4 as alternative counter electrodes in dye-sensitized solar cells

Anurag Roy,[1,2] Parukuttaymma Sujatha Devi,[1,a] Smagul Karazhanov,[3] D. Mamedov,[3] Tapas Kumar Mallick,[2] and Senthilarasu Sundaram[2,a]
[1]*Sensor and Actuator Division, CSIR-Central Glass and Ceramic Research Institute, Kolkata 700032, India*
[2]*Environment and Sustainability Institute, University of Exeter, Penryn Campus, Cornwall TR10 9FE, United Kingdom*
[3]*Department for Solar Energy, Institute for Energy Technology, 2007 Kjeller, Norway*

(Received 6 May 2018; accepted 2 July 2018; published online 24 July 2018)

A contribution of counter electrode (CE) emphasis a great impact towards enhancement of a dye-sensitized solar cell's (DSSC) performance and Pt based CE sets a significant benchmark in this field. Owing to cost effective noble metal, less abundance and industrial large scale application purpose, an effective replacement for Pt is highly demanded. There are several approaches to improve the performance of a CE for enhancing the power conversion efficiency with a less costly and facile device. To address this issue, reasonable efforts execute to find out suitable replacement of Pt is becoming a challenge by keeping the same electrochemical properties of Pt in a cheaper and eco-friendlier manner. With this, cheaper element based quaternary chalcogenide, Cu_2ZnSnS_4 (CZTS) becomes a prominent alternative to Pt and used as a successful CE in DSSC also. This review presents brief discussion about the basic properties of CZTS including its synthesis strategy, physicochemical properties and morphology execution and ultimate application as an alternative Pt free CE for a low cost based enhanced DSSC device. It is therefore, imperative for engineering of CZTS material and optimization of the fabrication method for the improvement of DSSC performance. https://doi.org/10.1063/1.5038854

I. INTRODUCTION

The prosperity of human society largely relies on safe energy supply, and fossil fuel has been serving as the most reliable energy source. Human activities are closely dependent on the use of several forms and sources of energy to perform work. The energy content of an energy source is the available energy per unit of weight or volume, and the challenge is to effectively extract and use this energy without significant losses in conversion, transportation or utilization.[1,2] Thus, the more the energy consumed, greater is the amount of work accomplished. By implication the economic development is thus directly correlated with greater levels of energy consumption. However, as a non-renewable energy source, the exhaustion of fossil fuel is inevitable and imminent in this century. To address this problem, renewable energy especially solar energy has attracted much attention, because it directly converts solar energy into electrical power leaving no environment affect. Renewable energy is the energy derived from the available sources can be tapped from sun, wind, ocean, hydropower, biomass, geothermal resources, biofuels and hydrogen derived from renewable resources.[3,4] Renewable energy resources are available in wide geographical areas, in contrast to other energy sources, which are concentrated in a limited number of countries. Rapid deployment

[a]Corresponding Author Email: psujathadevi@cgcri.res.in, s.sundaram@exeter.ac.uk Telephone: +91-33-2483-8082, +44 (0) 1326 259486

of renewable energy and technological diversification of energy sources would indeed result in significant energy security and economic benefits. Among all the renewable energy forms, solar energy has showed its advantages and potential for power generation. This field is growing fast; it can be seen from Fig. 1(a) that the publications on "solar cells" increased according to the literature search based on ISI Web of Science and WIOP (2017).[5] As compared to silicon-based and thin-film solar cells, the third-generation solar cells such as dye-sensitized solar cells (DSSCs) and perovskite solar cells (PSCs) have the potential for a lower processing cost in the emerging PV fields. Reports on integrated devices based on DSSCs are more numerous as compared to PSCs based on the maturity of the DSSC technology. To date, the DSSC technology excels with inherent low toxicity, low cost, and increased long-term stability which has been realized by commercially also. Recently, PSCs have paid much attention due to its highly scalable and integrated photovoltaic performance over DSSCs and as a result it appears as a strong contender in terms of publications for DSSCs. The development of the device configuration can generate a key advance in cell efficiency and fabrication process of PSCs, from DSSCs, was accompanied by a dramatic advance in photo-current conversion efficiency (PCE). Although the cell efficiencies of the third-generation solar cells are at present still lower than those of silicon-based and thin-film solar cells, the total cell efficiency of the tandem devices combining PSCs with silicon based solar cells is expected to exceed Shockley-Queisser limit in the near future.

The main obstacle for harvesting of solar energy in large scale is that the existing photovoltaic devices do not exhibit high enough solar to electric power conversion efficiencies with both cost effectiveness and necessary longevity which promotes the researchers to take new initiatives for harvesting incident solar photons with greater efficiency and economical endurance. Among the various solar cells, dye-sensitized solar cells (DSSCs) have attracted much attention because of its low cost, facile fabrication, faster energy payback time and diverse modification.[6–9] The basic aim of DSSCs lies on higher solar to electricity conversion efficiencies with lower production costs, flexibility and eco-friendliness. The key idea of the technology being photoelectrochemical in nature closely resembles with natural photosynthesis process. Like chlorophyll in plants, a monolayer of dye molecules (sensitizer) absorbs the incident light, giving rise to the generation of positive and negative charge carriers in the cell. DSSC provides a technically and economically credible alternative concept to present day p-n junction photovoltaic devices. A DSSC device can basically constructed with semiconducting oxide/sensitizer/electrolyte/counter material combined photoelectrochemical cell. So an efficiently functional device can only be achieved by proper selection of semiconducting oxide/sensitizer/electrolyte/counter material through which the loss of electron rather current could be effectively minimized. Many research experiments have been made for DSSCs in order to achieve high-performance devices.[10] Each component of the cells vitally influences the cost, cell performance and durability. Therefore, in the past years, the materials used in DSSCs have

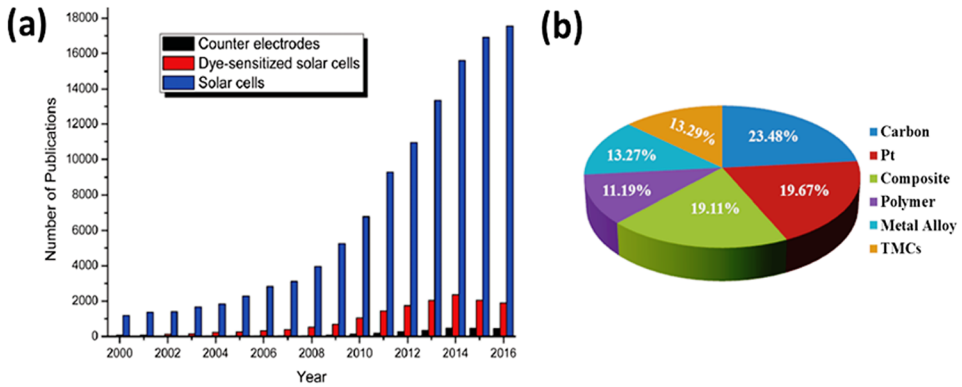

FIG. 1. Number of (a) published articles and (b) percentage of article published by keyword carbon, Pt, composite, polymer, metal alloy and TMCs on counter electrodes in dye sensitized solar cells as obtained from ISI Web of Science and WIOP (World Intellectual Property Organization, 2017).

experienced rational design and careful modification including the fabrication of nanostructured semiconductor photoanodes with effective dye loading and fast electron transport, the synthesis of versatile quantum dots (QDs) with high absorption coefficients and appropriate band gaps to maximize light harvesting, the preparation of redox electrolytes with strong capacity for efficient hole transport and long-term stability, and the formation of various CEs with high electrocatalytic ability in reduction of the oxidized electrolyte. Usually Pt nanoparticle coated on fluorine doped SnO_2 (FTO) glasses as obtained by thermal decomposition, sputtering or chemical reduction is used as the counter electrode. Pt counter electrode is very efficient in I^-/I_3^- redox regeneration (the conversion of I_3^- to I^- occurs on the surface of Pt) which in turn helps in the regeneration of oxidized dye. Thus, platinum acts as catalyst for the charge transfer reaction occurring between iodide and tri-iodide. However in view of the high cost and scarcity of Pt, significant efforts are directed towards replacement of this Pt catalyst with other low cost, earth abundant, non-toxic materials.[11–13]

Based on the above selection criteria, potential of many materials have been evaluated for applications as the CE of DSSC, and good progress has been achieved. Some of the novel CE materials exhibit properties that are more advanced than Pt and might be helpful to promote commercialization of DSSC. According to the material composition, the CEs can be made of Pt or other metals, carbon or transition metal compounds, conductive polymers, and composites. Although the classical highest efficiency is based TiO_2 as working electrode and Pt as counter electrode,[14–16] the highest photo-current conversion efficiency (PCE) ~ 9.33% is achieved in TiO_2/N719/Pt device in the presence of I^-/I_3^-electrolyte whereas the PCE is enhanced to 12.3% upon change in the dye with Y123-YD-o-c8 and electrolyte with Co^{2+}/Co^{3+}.[17,18] On the other side, Mathew et al. (2014) reported a till date highest PCE of 13% for a DSSC fabricated with TiO_2/molecularly engineered porphyrin dye/Graphene nanosheets in presence of Co^{2+}/Co^{3+} redox shuttle.[19] Each layer of DSSC determines the materials and fabrication cost. In the past years the researches have mostly focused on efficiency enhancement through modification of the major components of DSSC such as morphology of the oxide-based photoanode and counter electrode,[20–23] size control,[24] scattering layer,[25–27] surface treatment,[28,29] sensitization with various dyes[30–34] using of scattering layer over photoanode oxide, implementation of photoanode alternative to TiO_2, redox electrolyte, counter electrode, etc. The CE is an important part of a DSSC device. Reduction of the redox electrolyte and the collection of electrons received from the external load to the electrolyte is the active responsibility of a CE. Noble metals are more acceptable as a CE's due to its superior catalytic activity and faster redox property. Also, high conductivity for charge transport, good electrocatalytic activity for reducing the redox couple and excellent stability are the major contribution for choosing noble metal such as Pt, Au, Ag based CE.[35,36] However, as a noble metal, Pt becomes a trendsetter for applications as CE in DSSC that determines the main part of cost of the DSSC and limits its large scale applications. Superior catalytic activity, flexible electrochemical performance, good conductivity, high active area, cheaper and greener synthesis and fabrication techniques, effective performance is expected from CE alternative to Pt in DSSC. Recently graphene and other carbon based composites,[37–39] transparent metal compounds (TMC), metal sulfides (MoS_2, WS_2, NiS etc.),[40] transition metal carbides (TiC, WC, Mo_2C, SiC, ZrC etc.) and nitrides (TrN, ZrN, CrN, Fe_2N, Mo_2N etc.),[41,42] conducting polymers (polyaniline, polypyrole etc.),[43] ternary metal based sulfides or selenides like Cu_2ZnSnS_4 (CZTS), $Cu_2ZnSnSe_4$, Cu_2FeSnS_4, Cu_2NiSnS_4 etc.[44,45] exhibited performance that is competitive to Pt. The research has led to large increasing number of publications. Fig. 1(b) represents a pie chart represents publications under the topic of counter electrodes in DSSC. The high price and weak corrosion resistivity in liquid electrolyte are the other key concerns in the necessity to replace the Pt CEs with other materials. Today, several alternatives have been explored as replacement to Pt that is more advanced than Pt in catalytic activity, price, abundance, and durability. They are carbon, metal sulfide and oxide based, transition metal nitrides and carbides, polymers and carbon-polymer composites and other composites.[46–55] Remarkably, all the alternative CEs are established as a potential replacement to Pt in due course of its synthesis strategy, morphology-size tunable property, fabrication policy etc. The reported alternative CEs mainly concentrating on different synthesis processes which can lead to industrial scale manufacturing.

II. OBJECTIVE

CZTS is one of the very popular materials in inorganic thin films photovoltaic technology that consists of non-toxic, cheap and earth abundant elements Cu, Zn, Sn and S. In spite of thin film solar cell application, CZTS can be found as a recent approach towards non Pt based CE based research perspective.[56,57] CZTS based CEs are reported to exhibit better performance than Pt CE. Potential of CZTS for applications in DSSC as CE is relatively new. Reduction of the redox electrolyte and collection of photogenerated free electrons received from the external load to the electrolyte is the expected functionality from CE. This review will focus on the latest developments and highlights, challenges, and perspectives of using CZTS as CE in DSSC. At first, some basic information about physical and chemical properties of CZTS will be briefly addressed. The methods of synthesis of CZTS are the other important point that was well developed for applications as solar absorber in CZTS cells. This issue needs critical analysis in connection to the novel application as CE. First, the fundamental concept of the DSSC solar cells will briefly be reviewed. This will be followed by counter electrode role in a DSSCs and importance of CZTS. Subsequent sections are dedicated to the synthesis methods and available counter electrode materials for DSSC applications. In the next section the importance of the CZTS material including its structural and physico-chemical characterization will be highlighted. This will be followed by recent advances of CZTS based counter electrode performance in terms of their fabrication technique, various morphology and great electrocatalytic activity for DSSCs will be highlighted. We aim to elaborate the rational strategies in CZTS counter electrode development in DSSC applications.

III. FUNDAMENTALS OF DYE SENSITIZED SOLAR CELLS

Helmut Tributsch and Melvin Calvin had mimicked this phenomenon of photosynthesis process by utilizing the electrochemical properties of chlorophyll in an extra cellular environment for the generation of electricity from sunlight which brought forth the DSSC device.[14–16] DSSC usually contains photoanode, sensitizer (dye), electrolyte and counter electrode (CE) material, as shown in Fig. 2. It is a sandwich device assembled of two electrodes and electrolyte producing electrical current through redox reactions upon illumination of sunlight. Both electrodes are placed parallelly to each other and the electrolyte is sandwiched between them. A monolayer of the light-sensitive charge transfer dye has been further attached to the semiconducting oxide film. The electrically conducting glass substrate coated with a thin layer of Pt catalyst acts as the counter electrode. This has been placed parallel with a face to face configuration to the working electrode. The interspacing has been filled with the liquid or solid electrolyte that plays a role of conducting media.[14] The example of design of a complete DSSCs device has been illustrated in Fig. 2. The light-absorbing dye molecules attached to the semiconducting metal oxide (SMO) surface plays a role

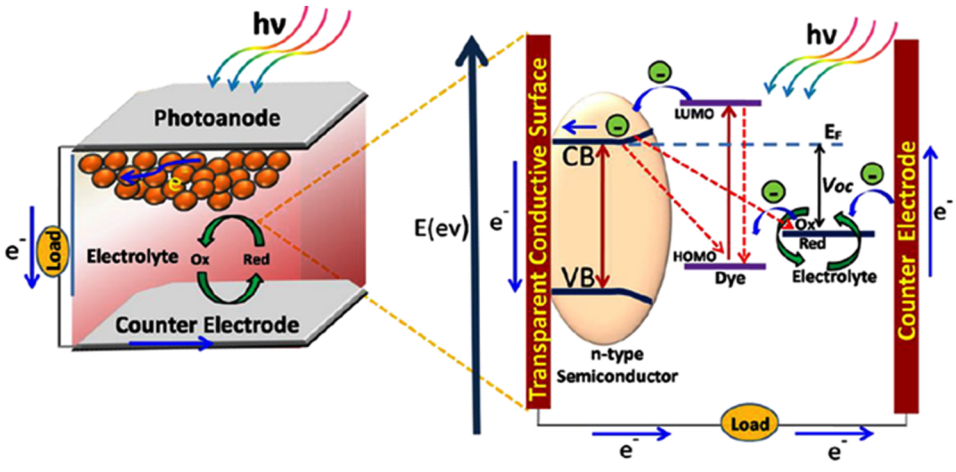

FIG. 2. Schematic representation of the working principle of a DSSC device.

of sensitizer.[58] The thin layer of platinum coated on conducting glass acts as the CE. Upon illumination by the sunlight, the dye molecules absorb photons of wavelength equal to or exceeding the energy difference between its highest occupied molecular orbital (HOMO) and lowest unoccupied molecular orbital (LUMO). Electrons from the ground electronic state of dye get promoted to the excited state, the so-called photoexcitation of dye, which is equivalent to the electron injection to the conduction band (CB). These photoexcited free electrons are then transported through the semiconductor by diffusion to reach the transparent conducting layer deposited on the glass substrate. The iodide ion (I^-) then donates electron to the oxidized dye at anode and regenerates the dye molecules. The oxidized (ox) species of electrolyte i.e. triiodide (I_3^-) in iodide-triiodide (I_2/I_3^-) complex, is reduced to iodide at the cathode. The above processes go in cycle. As a consequence electrical current flow continues through the external circuit as long as the sunlight is incident on the cell.

In DSSCs, the transportation of charge carriers from the photoanode to the CE meets various electrical resistances, including: the series resistance (R_S) comprising the sheet resistance of TCO/glass and the contact resistance of the cell; the resistance at TCO/SMO contact ($R_{TCO\text{-}SMO}$); the transport resistance of electrons in the SMO film (R_{SMO}); the charge-transfer resistance of the charge recombination between the electrons in the SMO film and I_3^- in the electrolyte (R_{CT}); the Warburg parameter describing the Nernst diffusion of I_3^- in the electrolyte; the charge-transfer resistance at the CE/electrolyte interface ($R_{CE\text{-}electrolyte}$); and the charge-transfer resistance at the exposed TCO/electrolyte interface ($R_{TCO\text{-}electrolyte}$). In DSSCs, the charge-transfer resistance at the CE/electrolyte interface ($R_{CE\text{-}electrolyte}$) is often dominant among multiple charge-transfer resistances, and thus the R_{CT} often refers to $R_{CE\text{-}electrolyte}$, if there is no special note. Among these charge-transfer resistances, the series resistance (R_S) and the charge-transfer resistance at the CE/electrolyte interface (R_{CT}) are enslaved to the CEs. The series resistance of a solar cell dominates fill factor losses, especially in large area commercial solar cells. A smaller series resistance (R_S) will give a higher FF, which results in a high conversion efficiency.[59–61]

IV. ROLE OF COUNTER ELECTRODE

CE must be catalytically active possessing high electron collection efficiency from the external load to the electrolyte for its regeneration and reduce the overpotential of the device. As mentioned earlier, CE mainly promotes the electron transfer from the external circuit back to the electrolyte at the surface of CE/electrolyte interface and accelerates the electrolyte reduction.[35] Thus, the main function of a CE is to speed up I_3^- reduction towards I^-, which then regenerates the dye molecules. Therefore, CEs with the characteristics of both excellent electrocatalytic activity for I_3^- reduction and high electrical conductivity for electron transport are desirable. However, the CE materials do not exhibit both high electrical conductivity and catalytic activity at the same time. When the catalytic properties of the CE materials cannot sustain the required electrical current, the effective exchange current must be enhanced by increasing the CE surface area. As the higher surface area of the CE produces more catalytic sites for the electrolyte reduction, which is favorable for the regeneration of the dye sensitizer, imparting porosity to the catalysts, the supports, or both, is desirable for enhancing the catalytic activity of CEs. Generally, Pt has proven to be a good CE catalyst in liquid state DSSCs. However, for practical and economic considerations, a series of high-performance Pt-free CE materials are needed and particularly design to maximize its function and to meet the compatibility demands in a wider range of DSSCs containing alternative CE catalysts. Only in this case can those materials deposited on transparent conducting oxide-based (TCO) substrates be effectively utilized as a CE for DSSCs. It is difficult to maintain all such ideal parameters like 80% optical transparency at a wavelength of 550 nm, 20 Ω sq^{-1} sheet resistance (R_{SH}) and 2-3 Ω cm^2 charge transfer resistance (R_{CT}) for a single material.[62] Thus an effective strategy is to replace Pt coating layer on the surface of glass substrate with a highly active and cheaper hybrid materials, utilizing a combination of different materials in the design of CEs will likely produce synergetic effects that greatly enhance the relevant parameters for state-of-art CE operation. This strategy is very popular in exploiting alternative Pt electrode. Also, CE surface roughness affects the performance of the DSSC in the sense that as the surface roughness increases the conversion efficiency increases because the voltage drop on the

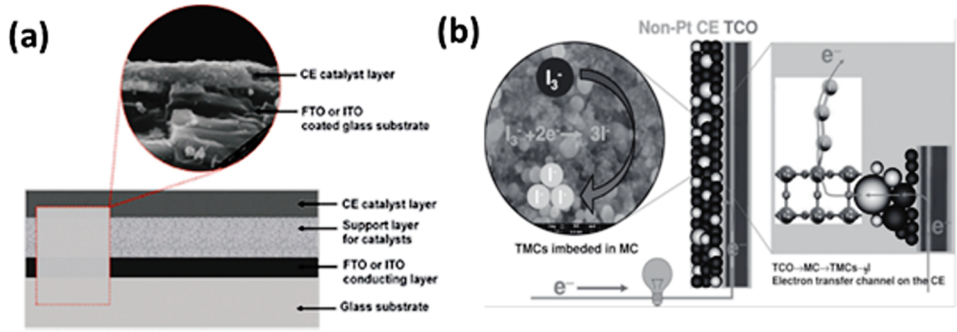

FIG. 3. (a) The structural sketch of hybrid counter electrode and (b) Schematic representation of the operation principle of a non Pt composite. "Reproduced with permission from Yun *et al.*, Adv. Mater. **26**, 6210 (2014). Copyright 2014 John Wiley and Sons".

counter electrode decreases. Operational principle of a non Pt based CE, such as mesoporous carbon (MC) and TMC has been illustrated in Figs. 3(a)–(b).

As the larger is the counter electrode area, the larger is the surface for the electrochemical reaction and consequently the larger is the electrode current for the same voltage drop on the electrode.[63] It is also important to deal with the electrochemical impedance spectroscopy (EIS) analysis to select a CE for DSSC application. EIS reveals also the information about electrode/electrolyte interface. Catalytic properties of CE can be studied by measuring the charge transfer resistance (R_{CT}) between the electrode and the electrolyte. To determine the R_{CT} of CE, a symmetric CE-electrolyte-CE device is often used in order to give more detailed description of the CE by eliminating the photoanode effects. Typical impedance spectra of a symmetric dummy cell and its equivalent circuit are revealed by a Nyquist plot which depicts the change in R_{ct}. R_S represents the total ohmic resistance offered by the two electrodes and the electrolyte. A systematic flow chart, as shown in Fig. 4 describes about the materials synthesis, characterization and performance evaluation to be an active non Pt based CE for DSSC.

In case of the CZTS-based DSSC, a plausible electron transfer mechanism has been illustrated in Fig. 5(a).[64] The open-circuit voltage, V_{OC} (0.7-0.8 V) is usually governed by the Fermi energy around the CB (E_{CB}) of TiO_2 (E_{CB}: -0.5 V vs normal hydrogen electrode (NHE)), and the oxidation reduction potential of I^-/I_3^- (0.33 V vs NHE) in case of a conventional DSSCs device.[64] However, V_{OC} of the TiO_2/CZTS DSSCs is determined by the quasi-Fermi levels above the VB of CZTS and below the CB of TiO_2. In many cases of p-type bulk semiconductors, the flat band potential (E_{FB}) from the

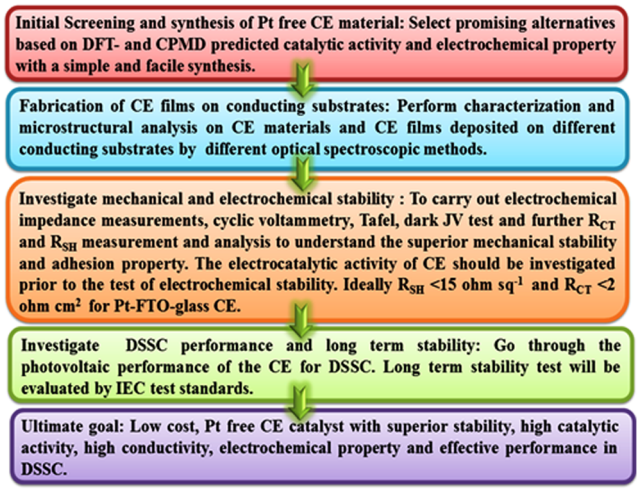

FIG. 4. Flow chart of Non-Pt based CE selection, preparation, characterization and performance study.

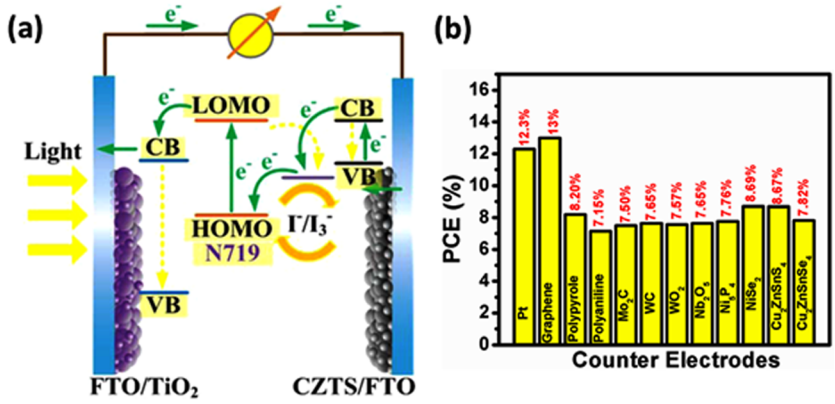

FIG. 5. (a) CZTS used as CE in DSSCs. "Reproduced with permission from Chen *et al.*, ACS Sustainable Chem. Eng. **3**, 2652 (2015). Copyright 2015 American Chemical Society". and (b) significant power conversion Efficiency (PCE) of different counter electrodes used in DSSC.

current-voltage curve of the photocurrent response can be comparable to VB. In Fig. 5(a) the green arrows signifies the possible electron transfer, and the dashed yellow arrows indicate the possible electron recombination. In overall, high catalytic activity and flexible electrochemical properties leads to set a CE material for DSSC. It also becomes a challenge for the CE with respect to Pt in DSSC to produce higher efficiency. Therefore, many studies have been carried out to reduce the amount of Pt in DSSCs and/or to explore alternatives to Pt. Remarkably, some new catalysts behave better than Pt for

TABLE I. Significant performance of various counter electrode materials (Pt and non-Pt based) in DSSC.

Type of Counter	Counter Material	Efficiency (%)	Reference
Pt based	Pt	6.91	66
	$Pt_{0.02}Co$	10.23	67,68
	Pt_3Ni	8.78	69
	PtPd	7.45	70
	PtAu	3.40	71
	PtCuNi	9.66	72
	PtCoNi	8.85	73
	Pt/NiO/Ag	11.27	74
Carbon Based	Carbon Black Nanoparticle	9.1	75
	Carbon Nanofibre	7.0	76
	Pt/Carbon Nanofibre	9.4	77
	Graphene	13	19
	N, P doped Graphene	8.57	78
	I-Graphene Nanoplatelets	10.31	79
	Au-Graphene Nanoparticle	14.30	80
	Graphite	7.67	81
	Polyaromatic Hydrocarbon	8.63	82
Polymer Based	Transparent PEDOT	8.00	83
	Polyaniline Nanowire	8.24	84
	Polypyrole	7.73	85
Transition Metal Based	TiN	7.45	86
	Mesoporous WC	8.23	87
	FeN/N doped Graphene	9.93	88
	MoS_2	6.82	89
	CoS	8.12	90
	$CoSe_2$	8.15	91
Hybrid	PEDOT:PSS/Graphene	7.31	92
	Fe_3O_4@RGO-NMCC	9.46	93

new redox couples (or hole conductors). This highlights the importance of a proper match between CE catalysts and redox couples. This relationship must be considered in the process of developing new CE catalysts or new redox couples. A comparative performance of some significant performance of available CEs in DSSC is shown in Fig. 5(b).[48,49,65] Table I highlighted about some significant performance of various counter electrode materials available for DSSC application.[66–93]

V. CHEMICAL IDENTITY OF Cu_2SnZnS_4

In contrast to common oxides, CZTS, as a direct band gap semiconductor, has the band gap energy of ~1.4-1.5 eV and is close to the optimal band gap energy of 1.45 eV. In addition, CZTS has a high absorption coefficient $>10^4$ cm^{-1} along with intrinsic *p*-type conductivity of CZTS also makes it a suitable CE due to the fast transfer of photo-generated holes and further efficiency.[94–96] CZTS nanocrystal-based approaches start with the controlled synthesis of nanocrystals and end with the deposition and post treatment of films. CZTS thin films have been prepared by various methods such as spray, thermal evaporation, and spin for solar cell applications. Chen et al. (2016) recently reported a highest efficiency of 8.67% by using the semi-transparent two dimensional leaf-like CZTS plate arrays *in-situ* growth on a FTO glass substrate without going any post-treatment.[97] The overall PCE of CZTS CE's are still lesser than the Pt and carbon based CE materials and further studies like fabrication technique, synthesis strategies, doping, tuning of optical properties are also need to be monitor for improved performance of the CZTS based CE (Fig. 5(b)). In this review, we have highlighted glimpse of such methods towards effective performance as a low cost material based CZTS CE which can highlights the possibility to use as an alternative to Pt CE in DSSC. At the same time, implementation of CZTS CE could pave way to future developments in the area of DSSCs. With this, becoming a non Pt based material, a thorough study on the recent performance of CZTS based CEs are also included in this review later. At the same time we have focused on the performance evaluation of synthesis, morphology and fabrication of CZTS films for DSSC in this review. We have also highlighted over phase purity, synthesis strategy, morphology variation and film fabrication developments of CZTS CEs and its performance towards DSSC. As a non Pt based material, the quaternary chalcogenide complex CZTS has effectively becomes a significant replacement and with this here we are reporting also the physicochemical properties of cheaper CZTS towards the extraordinary performance of a successful replacement of costly Pt.[98] The chemical states of the elements in the CZTS material in the depth direction were studied to identify the presence of secondary phases, which are detrimental to the performance of solar cells containing CZTS. A quaternary chalcogenide, CZTS is an emerging solar cell material having earth-abundant, low toxic and low cost elements, near-optimum direct band gap energy of ~1.5 eV and a large absorption coefficient ($>10^4$ cm^{-1}). The crystalline structure of CZTS consist the chalcopyrite structure which indicating that its unit cells can be obtained from the chalcopyrite structure by substituting half of the indium atoms with zinc atoms and the other half with tin atoms. CZTS can be crystallized in kesterite (KS), stannite (ST), or primitive mixed Cu-Au (PMCA) structural arrangements (Fig. 6).[9]

KS and ST structures are body-centered tetragonal and may be thought of as two sulfur face-centered cubic (fcc) lattices stacked on top of each other with Cu, Zn, and Sn occupying half the

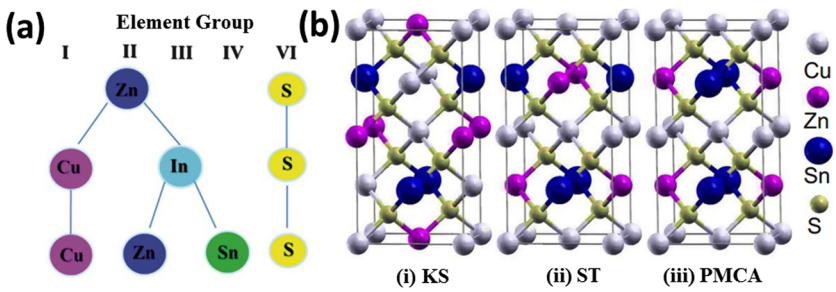

FIG. 6. (a) Schematic of elemental position representation of CZTS and (b) (i) kesterite (KS), (ii) stannite (ST) and (iii) primitive mixed Cu-Au (PMCA) crystalline structure of CZTS lattices. "Reproduced with permission from Chen *et al.*, Appl. Phys. Lett. **94**, 041903 (2009). Copyright 2009 AIP Publishing LLC".

tetrahedral voids within this FCC lattice. The PMCA structure is primitive tetragonal. The differences in the arrangement and stacking of the metal cations within the tetrahedral voids give rise to these three different structures. Specifically, the KS structure consists of two alternating cation layers each containing Cu and Zn or Cu and Sn, whereas in the ST and PMCA structures, a layer of Cu alternates with a layer of Zn an In the ST structure, the Zn and Sn atoms on the same layer switch their positions every other layer. This location swapping between Zn and Sn, every other layer, is absent in PMCA, which makes it primitive tetragonal and distinguishes it from the ST structure. In all these structures, the sulfur FCC sublattice determines the unit cell dimensions, and the X-ray diffraction (XRD) is not sensitive to the metal cation arrangement. As a result, within experimental broadening of the diffraction peaks, it is a challenge to differentiate between KS, ST, and PMCA structures using XRD. Similarly, it is difficult to distinguish XRD peaks corresponding to CZTS, ZnS, and SnS. There are other unwanted secondary phases are also derived as ZnS, Cu_2S, SnS_2, Cu_2Sn_3 etc. during the synthesis of CZTS nanocrystals. Therefore, development of phase pure CZTS crystals are significantly depending on the methods used to prepare the material.[99–106] As it was reported in theoretical studies of CZTS by the effective medium theory, the secondary phases of Cu_2S, SnS can cause engineering of the band gap and will influence on light absorption properties of the material.[107] Depending on fill factor of some of the secondary phases, intermediate bands can be formed also.[108] Similar intermediate bands can be observed in the CZTS-SnS_2 system also.[108] The secondary phases play important role in electrical conductivity of CZTS At large concentrations of the secondary phases of ZnS and SnS_2 p-n junction might be formed that is localized around the secondary phase. These secondary phases might cause large scatter in not only in band gap and light absorption, but also in charge carrier lifetime, concentration and mobility. Thus, they can play key role in device performance. This unwanted secondary phase in CZTS can avert the DSSC performance. The chemical composition of CZTS thin films can be controlled fairly well by simply varying the concentration of the precursor solution. Table II summarizes the secondary phases developed during the synthesis or post treatment of CZTS which are also bearing significant physicochemical characters to interrupt the overall efficiency.[109]

There is a competition between phase pure CZTS growth and the growth of binary [Cu_2S, ZnS, SnS, and SnS_2] and ternary phases [Cu_2SnS_3] counterparts as the material itself possessing complexity of this quaternary complex due to having three metal cation and one metal anion. The CZTS phase formation is more complex and narrow in phase stability, as seen in Fig. 7.[65–68] Just et al. (2016) has investigated secondary phase formation and their influence in the formation of kesterite phase of CZTS by X-ray absorption near edge structure (XANES) analysis at the chalcogen K-edges. X-ray absorption near edge structure which enables the quantification of secondary phases

TABLE II. Various properties of secondary phases observed in CZTS materials. "Reproduced with permission from Kumar *et al.*, Energy Environ. Sci. **8**, 3134 (2015). Copyright 2015 The Royal Society of Chemistry".

Properties	CZTS	ZnS	Cu_2S	SnS	CuS	SnS_2	Cu_2SnS_3
Band gap (eV)	~1.45	~3.54-3.68	~1.21	1.3-1.4	2.5	~2.2	0.98-1.35
Electrical Properties	p-type Semiconductor	Insulator	P-type, metal like, highly defective	p-type high optical absorption co-efficient	p-type semiconductor Moderate conductor for electricity	n-type	p-type
Structure	Kesterite	Sphalerite and Wurtzite	Chalcocite	Orthorhombic	Hexagonal	Rhombohedral	Cubic and Tetragonal
Impact on Solar Cell	Essential absorbing material	Insulating, reduces device active area	Metallic and short solar cell	Non-toxic thin absorber layer low open circuit voltage	semi-metallic nature tendency to degrade the open circuit voltage, lower fill factor	Forms diode and barriers for carrier collections	Affects carrier collection efficiency

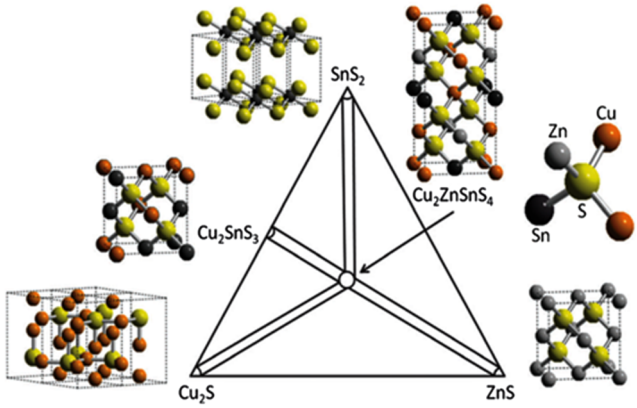

FIG. 7. The pseudoternary phase diagram to form the CZTS phase and other secondary phases along with their crystal structures. "Reproduced with permission from Du *et al.*, J. Appl. Phys **115**, 173502 (2014). Copyright 2014 AIP Publishing LLC".

in phase mixture systems by linear combination analysis.[110] Zhang et al. (2017) also monitored secondary phase formation CZTS by using the first principles calculations. This study reflects a significant analysis on deep electron traps defects inside CZTS and on the interface between CZTS and ZnS, largely reducing the efficiency of CZTS solar cell.[111,112]

VI. CURRENT TREND OF Cu_2SnZnS_4 BASED COUNTER ELECTRODES

CZTS CEs are finally implemented as an alternative, Pt free electrode in DSSC and their performance in the basis of varieties of synthesis techniques, morphology and film fabrication process are summarized in Table III.[45,55,64,97,100,112–124]

Performance of CZTS could be enhanced after treatment with $TiCl_4$, making composite with another alternative electro-catalysts such as graphene, carbon or may be variation in the precursor concentration or film deposition mechanism. In situ fabricated CZTS film was shown periodic deposition upon tuning the concentration of CZTS precursor and ethanol during solvothermal synthesis process and designated as CZTS 1,2,3 4, and 5. The digital image of the fabricated films was shown in Fig. 8(a) as executed by Chen et al. (2015).[64] The same film was further taken for $TiCl_4$ treatment which has increased the surface roughness of the substrate by forming a thin TiO_2 seed layer, and it is beneficial to generate an even film with strong contact with the FTO substrate (Fig. 8(b)).[64] *In-situ* growth CZTS nanoleaf based CE shows till now a highest efficiency of 8.67% as reported by Chen et al. (2016).[97] This highest efficiency achieved might be due to high catalytic surface area, fast photo-generated electron transport at the CE/redox electrolyte interface, remarkable electrocatalytic activity for I_3^- reduction, low charge transfer resistance toward the reduction of I_3^- ions, and high diffusion coefficient of the I_3^- even without any post-treatments and schematically represented in Fig. 8(c). The microstructure images of the same film have been illustrated in Fig. 8(d)–(g).[97] This result remarkably proves that CZTS can be a better alternative in replacement of Pt.

As mentioned, leaf like CZTS exhibits the maximum efficiency of 8.67% which is ~44% enhanced efficiency than Pt used CE under the same condition as shown in Fig. 9(a).[51] Inset of the same plot, a schematic of CZTS based DSSC system has also been given. The EIS study further elucidate about the catalytic activity of the different synthesized CZTS with Pt in the presence of I_3^-. In Fig. 9(b), a comparable R_{SH} of CZTS-6h (4.98 $\Omega.cm^{-2}$) to Pt (4.67 $\Omega.cm^{-2}$) reflects successful replacement of Pt in DSSC.[97] The small value of CZTS CEs indicates also a good bonding strength between in situ CZTS films and FTO substrates, which in turn promotes the transfer of more electrons from the external circuit or of holes from the electrolyte to the CEs. Solvothermally prepared CZTS films exhibited the highest efficiency of 5.65% than 4.96% by using Pt (4.96%) as alternative CE as reported by Chen et al. (2015),[125,126] corresponding *J-V* plot has been given as Fig. 9(c).[64] A typical Nyquist plot and equivalent circuit are illustrated in Fig. 9(d) of the same device in presence of iodine

TABLE III. Summary of the significant reports available on the performances of CZTS based counter electrodes according to its synthesis strategy, morphology and film fabrication process in DSSC.

Synthesis	Morphology	Efficiency (%)	Fill Factor (%)	Film Fabrication Method	Feature	Ref.
Hot-Injection method	Particle	6.47	57.00	Spin Coating	$Cu_2CoSn(SeS)_4$ and $Cu_2ZnSn(SeS)_4$	45
Hot-injection method	Particle	7.37	52.2	Spin Coating/ Drop Casting	Se introduction	55
In-situ hydrothermal	Nanosheet	5.65	63.00	*In-situ* direct film	$TiCl_4$ treatment	64
Electrodeposition/ Hydrothermal	Nanoleaf	8.67	51.07	Direct film through synthesis	*In-situ* growth method with green synthesis	97
Electrodeposition/ Solvothermal	Rounded Nanosheet	7.12	62.16	*In-situ* film growth	-	100
Solvothermal	Various	6.98	66.00	Zr based ball milled ink-spray casting	Morphology variation on $[Zn^{2+}]$	112
Ultrasonication	Microsphere	4.75	47.00	Spin Coating using EG	2% Graphene treated: 7.81%	113
Solvothermal	Particle	3.22	39.72	Drop casting using terpinol & EC	Substitute Se: 5.75%	114
DC magneton Sputtering	Particle	7.94	62.00	Direct *In-situ* film	influence of the [Cu]/[Zn] + [Sn] molar ratio in the CZTS samples	115
Pulsed Laser Deposition	Nanoplate	3.65	55.00	Direct *In-situ* film		116
Electrospinning	Nanofibre	3.90	65.00	Direct deposition during electrospinning	Cellulose Acetate, PVP binder varied synthesis	117
Hot-Injection method	Particle	4.35	52.00	Spray coating	Used in QDSSC	118
Solvothermal	Polygonal NP	4.24	60.96	Spin coating	-	118
Mo-foil assisted solvothermal	Porous flake	1.23	68.8	*In-situ* direct film	Mo foil supported direct film	119
Hot-injection method	Particle	6.89	68.69	Wurtzite Structure	Phase depended application	120
DC-sputtering	Particle	5.90	57.60	Metal substrate growth	Different etching process	121
Sonication	Microsphere	3.73	41.00	Spin Coating	-	122
Spray Coating	Particle	6.40	53.00	-	-	123
Sintering	Large grain NP	7.43	67.54	Drop Casting		124

electrolyte. The R_{SH} value of CZTS and Pt demonstrates that the CZTS 3 electrode (4.41 ohm cm^{-2}) has a superior electrocatalytic activity as compared to that of Pt CE (10.67 ohm cm^{-2}) for I^-/I_3^- redox reaction with a smaller charge transfer resistance in electrolyte At the same time, the R_{CT} value of CZTS 3 electrode (2.40 ohm cm^2) is lower than that of Pt (3.83 ohm cm^2) further proving that these CZTS nanostructures are good candidates for Pt-free CE fabrication in DSSCs,. The lower value of R_{CT} signifies to an increase in the electro-catalytic activity of the CE, resulting in acceleration of the higher electron-transfer process at the electrolyte/CE interface.[64,115]

Partial replacement of S with Se could lead to the efficiency enhancement to 7.52 % as reported by Xin et al. (2011).[100] Kong et al. (2013) has also studied performance of CZTS according to synthesis of one pot route where wurtzite and kesterite both the phases are evaluated to understand the effect of phase purity towards CE application and wurzite phase of CZTS shows enhanced efficiency than kesterite even better than Pt.[120] Spray coated CZTS films are also capable to deliver effective replacement of Pt as reported by Swami et al. (2014).[123] An interesting result is also observed by Mali et al. (2014) where they have shown polyvinylpyrrolidone (PVP) based CZTS nanofibers synthesized

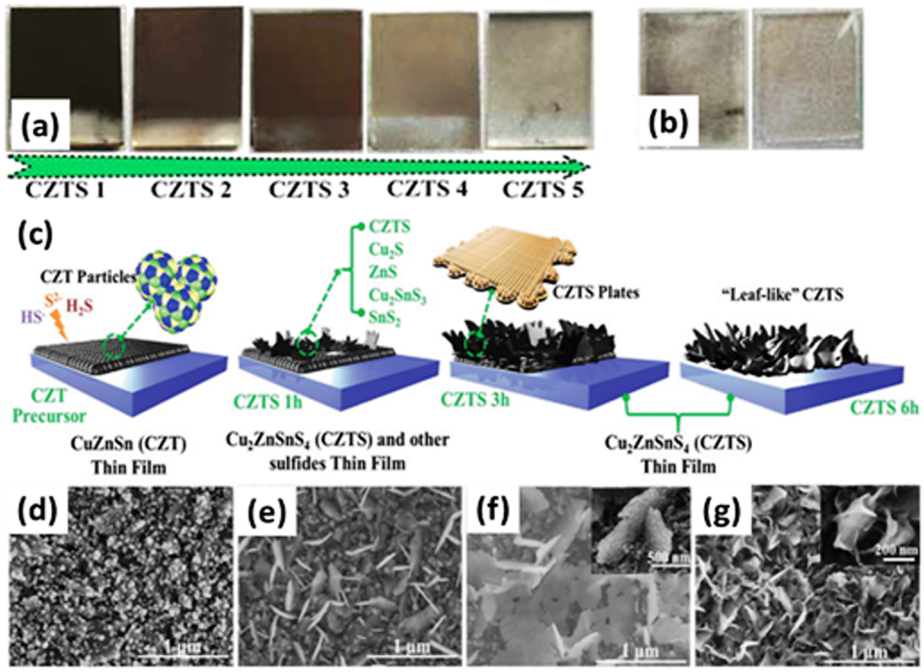

FIG. 8. (a) Digital images of the precursor concentration dependent solvothermally grown CZTS films, (b) Same films after $TiCl_4$ treatment, (c) Schematic illustration of the growth mechanism of the conversion process from CZTS particles to leaf-like CZTS plate arrays on the FTO substrate, FE-SEM images of the films of (d) CZT, (e) CZTS 1 h, (f) CZTS 3 h, and (g) CZTS 6 h. "Reproduced with permission from Chen *et al.*, Green Chem. **8**, 2793 (2016). Copyright 2016 The Royal Society of Chemistry".

by low cost electrospin technique is exceptionally better than same Pt as a CE.[117] With this, significant contribution reported by using CZTS CEs upon variation on different synthesis procedure and hence morphology along with *in-situ* film fabrication method of CZTS exhibits competitive performance as a suitable replacement of Pt as concise in Table III. Graphically, the FF is a measure of the "squareness" of the solar cell and is also the area of the largest rectangle which will fit in the *J* (current density) -*V* (voltage) curve. Therefore, in Table III we tried to compare all the reported efficiencies expand the possibilities for developing low-cost and scalable DSSCs by using CZTS based CE that dispose of the need for expensive and scarce Pt. Existing of multi phases causes low Voc, which is the major factor limiting the current efficiency of CZTS CE. On the other hand, a well-developed CZTS crystallites (and thin-film layers) have never exhibited tunable band gap(s). Therefore, one of the key effective recipes allowing the realization of high Voc as well tunable band gap is that doping and metal ion impregnation which can able to tune the opto-electronics property of the CZTS lattice without forming extra phases. On incorporation of Se in CZTS as CZTSSe, the band gap values are variable followed by enhancement of V_{OC}.[127] The high carrier concentration and low resistivity mean high electrical conductivity, which would result in the wurtzite CZTS that is more favorable when used as CE in DSSC. In addition to the aforementioned properties and performance evaluation, there are others various factors that must be taken into consideration when determine the most component DSSC.[128] With this theoretical screening study for more low-cost and high-efficiency CE materials are expected to be designed and fabricated through adjusting the local geometrical and electronic structures of certain functional materials. Recently, Kirubakaran et al. (2018) has developed CZTS counters using cost effective jet-nebulizer spray pyrolysis technique, exhibited an efficiency of 2.7%.[129]

VII. SYNTHESIS AND MORPHOLOGY EVALUATION OF Cu_2SnZnS_4

Ultrasonication, solvothermal, hot-injection method, electrospinning are the major synthesis strategy to prepare phase pure CZTS nanocrystals. On synthesis procedure and precursor alteration,

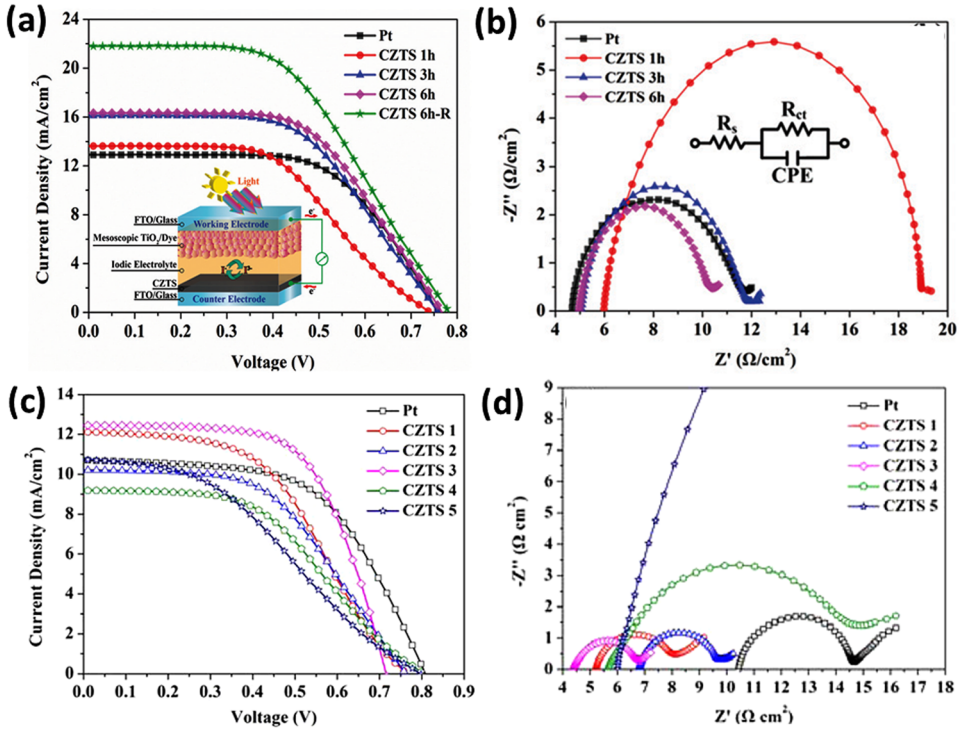

FIG. 9. (a) *J-V* characteristics of DSSCs with Pt and different transparent CZTS films as CEs under 100 mW/cm^2 for a DSSC device. The inset shows the schematic structure of the DSSC device by using semitransparent CZTS films as a CE, (b) Nyquist plots of impedance spectra for the I_3^-/I^- symmetrical cells based on Pt and corresponding equivalent circuit used for fitting. "Reproduced with permission from Chen *et al.*, Green Chem. **8**, 2793 (2016). Copyright 2016 The Royal Society of Chemistry." (c) *J-V* curves of the DSSCs with the films of various CZTS CEs on variation of CZTS precursor with commercial Pt measured under a light intensity of 100 mW/cm^2 and (d) corresponding Nyquist plots of impedance spectra. "Reproduced with permission from Chen *et al.*, ACS Sustainable Chem. Eng. **3**, 2652 (2015). Copyright 2015 American Chemical Society."

CZTS can alter its morphology according to that. It is important to deal with size, shape and morphology of the synthesized CZTS powders before implement to its CE application. For CZTS synthesis, as the solubility of intermediates decreases in the following order: ZnS > SnS > SnS_2 > CuS > Cu_2S ion exchange of pre-deposited ZnS with tin ion first and then copper ion could be favorable.[50] The final reaction could take place under heat treatment as per the equation (1),

$$ZnS + SnS_2 + 2CuS \rightarrow Cu_2ZnSnS_4 + S \quad (1)$$

Fig. 10 describes microstructural changes observed during FESEM analysis during the different synthesis procedure of CZTS. Highly mono dispersive nanocrystalline CZTS can be derived from hot-injection method as reported by Xin et al. (2011).[100] Xie et al. (2013) has already reported that tuning the morphology can directly affect performance of CE by variation of concentration of Zn^{2+} during the synthesis.[130] Besides that, variation of molar concentration of $[Cu^{2+}]/[Zn^{2+}]$ has also remarkably influence on the overall band gap, as reported by Tao et al. (2014).[131] In order to control the formation of the secondary phase, cations and anions are replaced with Fe, Mn, and Se in CZTS and the band gap and the micro structure of CZTS has also been studied.[132] A simplified synthesis strategy has been demonstrated for a range of quaternary chalcogenide nanoparticles of different quaternary/pentanary inorganic chalcogenides by thermolysis of metal chloride precursors using long chain amine molecules. In the synthesis aspects, Chen et al. (2016) has used sodium thiosulfate powders as the sulfur source, but not sulfur powders.[133]

Thiosulfate transforms H_2S and sulphate anion through disproportionation reaction where H_2S acts as an *in-situ* sulfide source of CZTS and sulphate anion functioning as a protective layer on the as prepared CZT precursor. Xiao et al. (2015) demonstrated that the low-toxicity 3-mercaptopropionic acid (MPA) can play an important role as an auxiliary ligand in the precursor solution during the

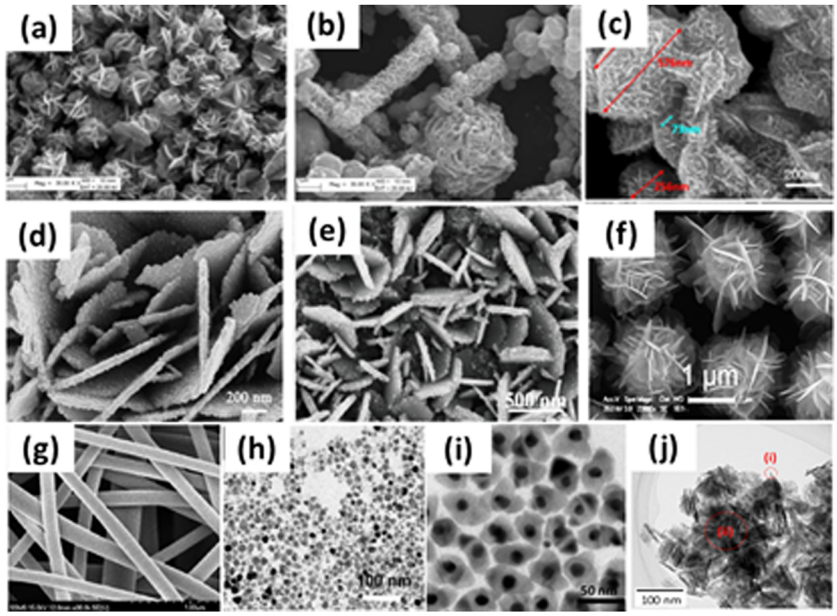

FIG. 10. (a)-(b) SEM images of the solvothermally prepared CZTS powders at 200°C for 48 h with Zn^{2+} concentrations of (a) 0.005, (b) 0.02, respectively. "Reproduced with permission from Xie *et al.*, RSC Adv. **3**, 23264 (2013). Copyright 2013 The Royal Society of Chemistry." (c) hierarchical metastable wurtzite CZTS microcrystals were successfully synthesized by a facile two-step heat-up route under the open-air condition. "Reproduced with permission from Qing *et al.*, Mater. Lett. **176**, 177 (2016). Copyright 2016 Elsevier." (d) CZTS microspheres "Reproduced with permission from Baia *et al.*, Mater. Lett. **112**, 219 (2013). Copyright 2013 Elsevier." (e) the rounded CZTS nanosheet. "Reproduced with permission from Chen *et al.*, Dalton Trans. **45**, 4513 (2016). Copyright 2016 The Royal Society of Chemistry." (f) CZTS microspheres. "Reproduced with permission from Xu *et al.*, J. Phys. Chem. C **116**, 19718 (2012). Copyright 2012 American Chemical Society". (g) PVP-CZTS nanofibre derived from electrospin method. "Reproduced with permission from Mali *et al.*, ACS Appl. Mater. Interfaces **6**, 1688 (2014). Copyright 2014 American Chemical Society". (h) bright field TEM images of CZTS nanocrystals. "Reproduced with permission from Xin *et al.*, Angew. Chem. Int. Ed. **50**, 11739 (2011). Copyright 2011 John Wiley and Sons". (i) Au@CZTS core-shell structure. "Reproduced with permission from Zhang *et al.*, Sci. Rep. **6**, 23364 (2016). Copyright 2016 Nature Publishing Group". and (j) CZTS nanorods. "Reproduced with permission from Miyauchi *et al.*, Phys. Chem. C **116**, 23945 (2012). Copyright 2012 American Chemical Society".

synthesis of CZTS which can avoid precipitation and noticeably improve stability of the precursor solution from ~3 hours to 1 week.[134] Coughlan et al. (2015) have investigated the evolution pathway of CZTS nanocrystals revealing that copper sulfide nanoparticles form in the early stages of the reaction before the progressive incorporation of tin and zinc to form stoichiometric CZTS by varying the copper precursor salt and amine concentration.[135] Plasmonic Au Nanoparticle core is actually helps to CZTS nanocrystalline shell in a core-shell mechanism manner to develop Au@CZTS core-shell nanostructures which actually enhance the efficiency of the device as reported by Zhang et al. (2015).[136] Expect disk, plates and particles nanorods can be also prepared by a facile solvothermal method as reported by Miyauchi et al. (2012).[137] Interestingly, CZTS in form of nanofibers has also been prepared by Mali et al. (2014) by electrospinning process using the polyvinylpyrrolidone (PVP) and cellulose acetate solvent separately.[117] A preferential crystallization along CZTS crystal direction around fiber surface was achieved by electrospinning method as reported by Mu et al. (2015).[138] Qing et al. (2016) developed a convenient and environment-friendly two-step heat-up method to fabricate pure phase wurtzite CZTS at relatively low temperatures under atmospheric condition.[139]

VIII. Cu_2SnZnS_4: VARIOUS FILM FABRICATION TECHNIQUES

Among the fabrication methods proposed above, in-situ direct film processing techniques of CZTS have shown their remarkable potential for constructing low-cost, large-scale, and high-performance DSSCs. Spin coating, spray coating, DC sputtering, successive ionic layer adsorption reaction (SILAR process), electrodeposition, hydrothermal/solvothermal direct processes are much

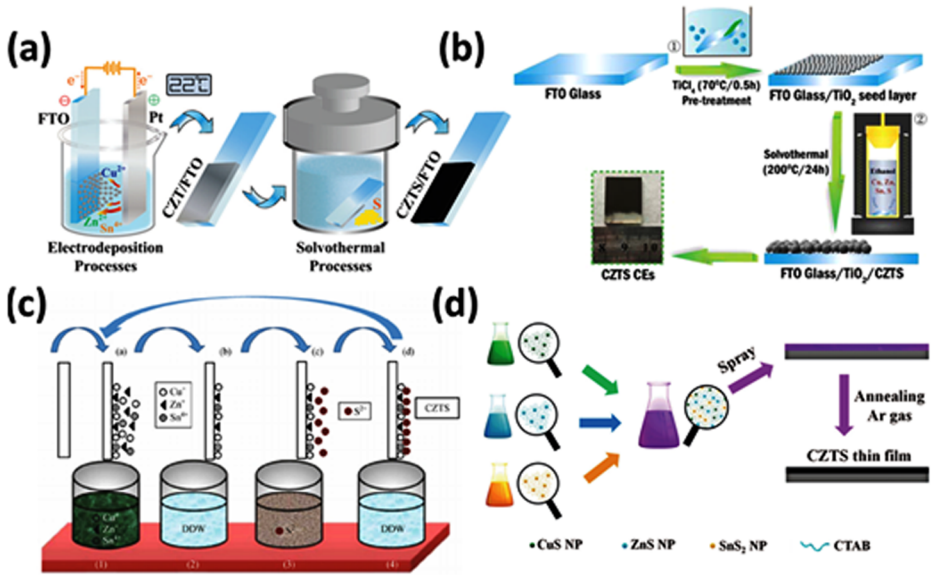

FIG. 11. (a) Schematic illustration of the fabrication processes of the CZTS counter electrode via electrodeposition and further solvothermal process. "Reproduced with permission from Chen *et al.*, Green Chem. **8**, 2793 (2016). Copyright 2016 The Royal Society of Chemistry." (b) Schematic illustration of the fabrication processes of the CZTS counter electrode. "Reproduced with permission from Chen *et al.*, ACS Sustainable Chem. Eng. **3**, 2652 (2015). Copyright 2015 American Chemical Society." (c) Schematic diagram of SILAR technique for the deposition of CZTS: beaker 1 contains cationic precursors, beaker 3 contains anionic precursor and beakers 2 and 4 contain double distilled water (DDW). "Reproduced with permission from Shinde *et al.*, Mater. Res. Bull. **47**, 302 (2012). Copyright 2012 Elsevier." (d) Schematic diagram of the preparation of CZTS solution using metal sulfides with cetyltrimethyl ammonium bromide (CTAB) as the capping ligand. "Reproduced with permission from Li *et al.*, RSC Adv. **4**, 26888 (2014). Copyright 2014 The Royal Society of Chemistry".

popular to deposit the CZTS layer over the FTO/ITO substrate directly. Spray deposited CZTS films are also prepared by Swami et al. (2014) that was further post-annealed in H_2S environment to improve the film properties.[123] Also, electrodeposited CZTS films have been fabricated by Chen et al. (2014).[140] They have used Reline as the green electrolyte to electrodeposite CZTS films for photovoltaic applications.

Guo et al. (2009) has developed nanocrystal ink of CZTS and applied it in the solar cells.[141] Spin coating technique,[142] screen printing,[143] DC sputtering[121] have been used to deposit CZTS based thin films. Suryavanshi et al. (2015) and Shinde et al. (2012) has reported SILAR processed CZTS thin film that can be used as CE in DSSC.[143,144] Chen et al. (2015) examined combination of $TiCl_4$ pretreatment and *in-situ* solvothermal growth to prepare the CZTS electrodes on FTO substrate.[64] Li et al. (2014) carried out CZTS film fabrication by an environment friendly way followed by binary sulfide nanoparticles were pre-synthesized in aqueous solution and then spray deposited onto glass substrates.[145] A simple and eco-friendly approach for preparing CZTS powders and screen-printing process was followed by Shen et al. (2013).[114] Various *in-situ* film fabrication processes have been schematically illustrated in Fig. 11. The above mentioned reports indicate that numerous processes can be successfully applied to deposit the CZTS based film.

IX. SUMMARY

Having several opportunities on prior modifications, DSSC offers significant non-conventional power production technique in an easier, cheaper, greener and clean technology aspect. Being considerable part of DSSC cell set up, counter electrode (CE) can play crucial role towards electron migration and redox cycle completion along with the sensitizer/electrolyte using in that concern cell. Due to having excellent stability and high catalytic activity Pt set up a benchmark as a CE for DSSC. But, due to uses of expensive noble metal and industrial scale up purpose it's a crucial requirement to set a prominent alternative of Pt. In due course, cheaper CZTS plays an effective replacement of Pt

and successfully implemented as an alternative CE in DSSC. This review summarize recent advances of CZTS based CE and their performance as an alternative material for costly Pt based CE for DSSC. These includes basic properties of CZTS, its different synthesis, morphological approach and lastly its potential application as an alternative CE towards an effective substitute of Pt in DSSC. Intense investigation should be done to develop more catalytic active, higher stability CZTS based CEs and for DSSC, and a new concept or design should be develop by in a cheaper way with environment friendly for clean technology and exhibit wide range of applications.

ACKNOWLEDGMENTS

AR gratefully acknowledge Department of Science and Technology (DST) for availing the Senior Research Fellowship of 2016-2017 under the INSPIRE program and DST and British Council for the Newton-Bhabha PhD Fellowship Award 2016-2017. SZK acknowledges financial support from the Research Council of Norway through the New Indigo project 237643 and M-ERA.net project 272806.

[1] S. Chu and A. Majumdar, Nature **488**, 294 (2012).
[2] A. S. Sánchez, E. A. Torres, and R. A. Kalid, Renewable Sustainable Energy Rev. **49**, 278 (2015).
[3] O. Ellabban, H. Abu-Rub, and F. Blaabjerg, Renewable Sustainable Energy Rev. **39**, 748 (2014).
[4] A. Kumar, K. Kumar, N. Kaushik, S. Sharma, and S. Mishra, Renewable Sustainable Energy Rev. **748**, 2434 (2010).
[5] J. Wu, Z. Lan, J. Lin, M. Huang, Y. Huang, L. Fan, G. Luo, Y. Lin, Y. Xie, and Y. Wei, Chem. Soc. Rev. **46**, 5975 (2017).
[6] K. Kalyanasundaram, *Dye-sensitized solar cells* (EPFL Press, United States, 2010).
[7] P. V. Kamat, J. Phys. Chem. C **111**, 2834 (2007).
[8] M. Grätzel, "Dye-sensitized solar cells," J. Photochem. Photobiol. **4**, 145 (2003).
[9] B. O'Regan and M. Grätzel, Nature **353**, 737 (1991).
[10] H. M. Upadhyaya, S. Senthilarasu, M.-H. Hsu, and D. K. Kumar, Sol. Energy Mater. Sol. Cells **119**, 291 (2013).
[11] M. Z. Iqbal and S. Khan, Sol. Energy **160**, 130 (2018).
[12] M. Ye, X. Gao, X. Hong, Q. Liu, C. He, X. Liu, and C. Lin, Sustainable Energy Fuels **1**, 1217 (2017).
[13] M. Ye, X. Wen, M. Wang, J. Iocozzia, N. Zhang, C. Lin, and Z. Lin, Mater. Today **18**, 155 (2015).
[14] H. Tributsch, Photochem. Photobiol. **16**, 261 (1972).
[15] A. Hagfeldt, A. G. Boschloo, L. Sun, L. Kloo, and H. Pettersson, Chem. Rev. **110**, 6595 (2010).
[16] A. Hagfeldt and M. Grätzel, Acc. Chem. Res. **33**, 269 (2000).
[17] V.-D. Dao and H.-S. Choi, Electrochim. Acta **93**, 287 (2013).
[18] A. Yella, H.-W. Lee, H.-N. Tsao, C. Yi, A. K. Chandiran, M. K. Nazeeruddin, E. W. G. Diau, C.-Y. Yeh, S. M. Zakeeruddin, and M. Grätzel, Science **334**, 629 (2011).
[19] S. Mathew, A. Yella, P. Gao, R. Humphry-Baker, B. F. E. Curchod, N. Ashari-Astani, I. Tavernelli, U. Rothlisberger, M. K. Nazeeruddin, and M. Grätzel, Nat. Chem. **6**, 242 (2014).
[20] Z.-S. Wang, H. Kawauchi, T. Kashima, and H. Arakawa, Coors. Chem. Rev. **248**, 1381 (2004).
[21] K.-M. Lee, V. Suryanarayanan, and K.-C. Ho, J. Power Sources **188**, 635 (2009).
[22] L.-L. Li, C.-W. Chang, H.-H. Wu, J.-W. Shiu, P.-T. Wu, and E. D. W. Diau, J. Mater. Chem. **22**, 6267 (2012).
[23] Z. Lan, J. Wu, J. Lin, and M. Huang, J. Mater. Chem. **223**, 948 (2012).
[24] K. G. Deepa, P. Lekha, and S. Sindhu, Sol. Energy **86**, 326 (2012).
[25] W. Xiang, D. Chen, R. A. Caruso, Y.-B. Cheng, U. Bach, and L. Spiccia, Chem. Sus. Chem. **8**, 3704 (2015).
[26] L. Zhu, Y. L. Zhao, X. P. Lin, X. Q. Gu, and Y. H. Qiang, Superlattices Microstruct. **65**, 152 (2014).
[27] H.-J. Koo, J. Park, B. Yoo, K. Yoo, K. Kim, and N. G. Park, Inorg. Chim. Acta **361**, 677 (2008).
[28] R. Liu, W.-D. Yang, and L.-S. Qiang, J. Pow. Sour. **199**, 418 (2012).
[29] X. Xin, M. Scheiner, M. Ye, and Z. Lin, Langmuir **27**, 14594 (2011).
[30] G. Richhariya, A. Kumar, P. Tekasakul, and B. Gupta, Renewable Sustainable Energy Rev. **69**, 705 (2017).
[31] T. Higashinoa and H. Imahor, Dalton Trans. **44**, 448 (2015).
[32] N. Santhanamoorthi, C.-M. Lo, and J.-C. Jiang, J. Phys. Chem. Lett. **4**, 524 (2013).
[33] J. G. K. Sumathy, Q. Qiao, and Z. Zhou, Renewable Sustainable Energy Rev. **68**, 234 (2017).
[34] S. Shalini, R. Balasundaraprabhu, T. Satish Kumar, N. Prabavathy, S. Senthilarasu, and S. Prasanna, Int. J. Energy Res. **40**, 1303 (2016).
[35] S. Yun, A. Hagfeldt, and T. Ma, Adv. Mater. **26**, 6210 (2014).
[36] J. Theerthagiri, A. R. Senthil, J. Madhavan, and T. Maiyalagan, Chem. Electro. Chem. **2**, 928 (2015).
[37] G. Veerappan, K. Bojan, and S.-W. Rhee, ACS Appl. Mater. Interfaces **3**, 857 (2011).
[38] D. W. Zhang, X. D. Li, H. B. Li, S. Chen, Z. Sun, X. J. Yin, and S. M. Huang, Carbon **49**, 5382 (2011).
[39] M. Chen and L. L. Shao, Chem. Eng. J. **304**, 629 (2016).
[40] W. Wu, Y. Wang, X. Lin, N. Yu, L. Wang, L. Wang, A. Hagfeldt, and T. Ma, Phys. Chem. Chem. Phys. **13**, 19298 (2011).
[41] M. Wu, X. Lin, Y. Wang, L. Wang, W. Guo, D. Qi, X. Peng, A. Hagfeldt, M. Grätzel, and T. Ma, J. Am. Chem. Soc. **134**, 3419 (2012).
[42] M. Wu, M. Sc, X. Lin, A. Hagfeldt, and T. Ma, Angew. Chemie. Int. Ed. **50**, 3520 (2011).
[43] K. Saranya, M. Rameez, and A. Subramania, Eur. Polym. J. **66**, 207 (2015).
[44] Z. Jin, M. Zhang, M. Wang, C. Feng, and Z.-S. Wang, Acc. Chem. Res. **50**, 895 (2017).
[45] F. Özel, A. Sarilmaz, B. İstanbullu, A. Aljabour, M. Kuş, and S. Sönmezoğlu, Sci. Rep. **6**, 29207 (2016).

[46] S. Thomas, T. G. Deepak, G. S. Anjusree, T. A. Arun, S. V. Nair, and A. S. Nair, J. Mater. Chem. A **2**, 4474 (2014).
[47] M. Wu and T. Ma, Chem. Sus. Chem. **5**, 1343 (2012).
[48] Q. Tang, J. Duan, Y. Duan, B. He, and L. Yu, Electrochim. Acta **178**, 886 (2015).
[49] S. Yun, P. D. Lund, and A. Hinsch, Energy Environ Sci. **8**, 3495 (2015).
[50] S. Ji and C. Ye, Rev. Adv. Sci. Eng. **1**, 42 (2012).
[51] H. Azimi, Y. Houac, and C. J. Brabecab, Energy Environ Sci. **7**, 1829 (2014).
[52] M. Wu and T. Ma, J. Phys. Chem. C **118**, 16727 (2014).
[53] L. Wang, M. Al-Mamun, P. Liu, Y. Wang, H.-G. Yang, H.-F. Wang, and H. Zhao, NPG Asia Mater. **7**, 1–15 (2015).
[54] M. K. Wang, N. Chamberland, J. Breau, J.-E. Moser, R. Humphry Baker, B. Marsan, S. M. Zakeeruddin, and M. Grätzel, Nat Chem. **2**, 385 (2010).
[55] M. Ye, X. Wen, M. Wang, J. Iocozzia, N. Zhang, C. Lin, and Z. Lin, Mater. Today **18**, 155 (2013).
[56] X. Liu, Y. Feng, H. Cui, F. Liu, X. Hao, G. Conibeer, D. B. Mitzi, and M. Green, Prog. Photovolt: Res. Appl. **24**, 879 (2016).
[57] G. K. Dalapati *et al.*, Sci. Rep. **7**(1350), 1–12 (2017).
[58] J. Bisquert, D. Cahen, G. Hodes, S. Rühle, and A. Zaban, J. Phys. Chem. B **108**, 8106 (2004).
[59] J. Halme, P. Vahermaa, K. Miettunen, and P. Lund, Adv. Mater. **22**, 210 (2010).
[60] Q. Wang, J.-E. Moser, and M. Grätzel, J. Phys. Chem. B **109**, 144945 (2005).
[61] A. Sacco, Renewable Sustainable Energy Rev. **79**, 814 (2017).
[62] J. E. Trancik, B. C. Barton, and J. Hone, Nano Lett. **8**, 982 (2008).
[63] S.-Q. Fan, B. Fang, J.-H. Kim, B. Jeong, C. Kim, J.-S. Yu, and J. Ko, Langmuir **26**, 13644 (2010).
[64] S. Chen, A. Xu, J. Tao, H. Tao, Y. Shen, L. Zhu, J. Jiang, T. Wang, and L. Pan, ACS Sustainable Chem. Eng. **3**, 2652 (2015).
[65] R. Irani, N. Naseri, and S. Beke, Coord. Chem. Rev. **324**, 54 (2016).
[66] Z. Zhang, S. Pang, H. Xu, Z. Yang, X. Zhang, Z. Liu, X. Wang, X. Zhou, S. Dong, and X. Chen, RSC Adv. **3**, 16528 (2013).
[67] B. He, X. Meng, and Q. Tang, ACS Appl. Mater. Interfaces **6**, 4812 (2014).
[68] B. He, X. Meng, Q. Tang, P. Li, S. Yuan, and P. Yang, J. Power Sources **260**, 180 (2014).
[69] J. Wan, G. Fang, H. Yin, X. Liu, D. Liu, M. Zhao, W. Ke, H. Tao, and Z. Tang, Adv. Mater. **26**, 8101 (2014).
[70] Q. Yang, P. Yang, J. Duan, X. Wang, L. Wang, Z. Wang, and Q. Tang, Electrochim. Acta **190**, 85 (2016).
[71] J. Han, K. Yoo, M. Ko, B. Yu, Y. Noh, and O. Song, Met. Mater. Int. **18**, 105 (2012).
[72] P. Yang and Q. Tang, Appl. Surf. Sci. **362**, 28 (2016).
[73] P. Yang and Q. Tang, Mater. Lett. **164**, 206 (2016).
[74] Z. Lan, L. Que, W. Wu, and J. Wu, J. Solid State Electrochem. **20**, 759 (2016).
[75] T. Murakami, S. Ito, Q. Wang, M. Nazeeruddin, T. Bessho, I. Cesar, P. Liska, R. Humphry-Baker, P. Comte, P. Pechyand, and M. J. Grätzel, Electrochem. Soc. **153**, A2255 (2006).
[76] J. Zhang, H. Long, S. Miralles, J. Bisquert, F. Fabregat-Santiago, and M. Zhang, Phys. Chem. Chem. Phys. **14**, 7131 (2012).
[77] F. Gong, H. Wang, X. Xu, G. Zhou, and Z. Wang, J. Am. Chem. Soc. **134**, 10953 (2012).
[78] C. Yu, Z. Liu, X. Meng, B. Lu, D. Cui, and J. Qiu, Nanoscale **8**, 17458 (2016).
[79] I. Jeon, H. Kim, I. Choi, K. Lim, J. Ko, J. Kim, H. Choi, M. Ju, J. Lee, and H. Kim, Nano Energy **13**, 336 (2015).
[80] K. Kakiage, Y. Aoyama, T. Yano, K. Oya, J. Fujisawa, and M. Hanaya, Chem. Commun. **51**, 15894 (2015).
[81] W. Lee, E. Ramasamy, D. Lee, and J. Song, ACS Appl. Mater. Interfaces **1**, 1145 (2009).
[82] B. Lee, D. Buchholz, and R. Chang, Energy Environ. Sci. **5**, 6941 (2012).
[83] J. Pringle, V. Armel, and D. MacFarlane, Chem. Commun. **46**, 5367 (2010).
[84] H. Wang, Q. Feng, F. Gong, Y. Li, G. Zhou, and Z. Wang, J. Mater. Chem. A **1**, 97 (2013).
[85] S. Jeon, C. Kim, J. Ko, and S. Im, J. Mater. Chem. **21**, 8146 (2011).
[86] Q. Jiang, G. Li, and X. Gao, Chem. Commun. **6720** (2009).
[87] J. Jang, D. Ham, E. Ramasamy, J. Lee, and J. Lee, Chem. Commun. **46**, 8600 (2010).
[88] J. Balamurugan, T. D. Thanh, N. H. Kim, and J. H. Lee, Adv. Mater. Interfaces **3**, 1500348 (2016).
[89] X. Yuan, X. Li, X. Zhang, Y. Li, and L. Liu, J. Alloys Comp. **731**, 685 (2018).
[90] J. Jia, J. Wu, J. Dong, Q. Bao, L. Fan, and J. Lin, J. Sol. Energy **151**, 61 (2017).
[91] S. Yuan, Z. Zhou, Z. Hou, W. Zhou, R. Yao, Y. Zhao, and S. Wu, Chem. Eur. J. **19**, 10107 (2013).
[92] H. Snaith, A. Moule, C. Klein, K. Meerholz, R. Friend, and M. Grätzel, Nano Lett. **7**, 3372 (2007).
[93] H. Zhou, J. Yin, Z. Nie, Z. Yang, D. Li, J. Wang, X. Liu, C. Jin, X. Zhang, and T. Ma, J. Mater. Chem. A **4**, 67 (2016).
[94] H. Matsushita, T. Ichikawa, and A. Katsui, J. Mater. Sci. **40**, 2003 (2005).
[95] C. Wang, S. Chen, J.-H. Yang, L. Lang, H.-J. Xiang, X.-G. Gong, A. Walsh, and S.-H. Wei, Chem. Mater. **26**, 3411 (2014).
[96] K. Ito and T. Nakazawa, Jap. J. Appl. Phys. **27**, 2094 (1988).
[97] S.-L. Chen, A.-C. Xu, J. Tao, H.-J. Tao, Y.-Z. Shen, L.-M. Zhu, J.-J. Jiang, T. Wang, and L. Pan, Green Chem. **8**, 2793 (2016).
[98] A. Polizzotti, I. L. Repins, R. Noufi, S.-H. Wei, and D. B. Mitzi, Energy Environ Sci. **6**, 3171 (2013).
[99] S. Chen, X. G. Gong, A. Walsh, and S.-H. Wei, Appl. Phys. Lett. **94**, 041903 (2009).
[100] X. Xin, M. He, W. Han, J. Jung, and Z. Lin, Angew. Chem. Int. Ed. **50**, 11739 (2011).
[101] X. Lu, Z. Zhuang, Q. Peng, and Y. Li, Chem. Commun. **47**, 3141 (2011).
[102] M. Quennet, A. Ritscher, M. Lerch, and B. Paulus, J. Solid State Chem. **250**, 140 (2017).
[103] K. Yu and E. A. Carter, Chem. Mater. **27**, 2920 (2015).
[104] A. Khare, B. Himmetoglu, M. Johnson, D. J. Norris, and M. Cococcioni, J. Appl. Phys. **111**, 083707 (2012).
[105] S. Levcenko, V. E. Tezlevan, E. Arushanov, S. Schorr, and T. Unold, Phys. Rev B **86**, 045206 (2012).
[106] S. Schorr, *Crystallographic aspects of Cu_2ZnSnS_4 (CZTS).copper zinc tin sulfide-based thin film solar cells* (Wiley Publishers, 2015).
[107] D. Mamedov, M. Klopov, and S. Z. Karazhanov, Mat. Lett. **202**, 70 (2017).

[108] D. Mamedov, Master thesis "Theoretical study of optoelectronic properties of kesterite modification of CZTS and solar cells," National Research Nuclear University, Moscow, Russia (2018).
[109] M. Kumar, A. Dubey, N. Adhikari, S. Venkatesan, and Q. Qiao, Energy Environ Sci. **8**, 3134 (2015).
[110] J. Just, C. M. Sutter-Fella, D. Lützenkirchen-Hecht, R. Frahm, S. Schorr, and T. Unold, Phys. Chem. Chem. Phys. **18**, 15988 (2016).
[111] Y. Zhang, K. Tse, X. Xiao, and J. Zhu, Phys. Rev. Mater **1**, 045403 (2017).
[112] H. Du, F. Yan, M. Young, B. To, C.-S. Jiang, P. Dippo, D. Kuciauskas, Z. Chi, E. A. Lund, C. Hancock, W. M. Hlaing, M. A. Scarpulla, and G. Teete, J. Appl. Phys. **115**, 173502 (2014).
[113] L. Baia, J. N. Ding, N. Y. Yuan, H. W. Hu, Y. Li, and X. Fang, Mater. Lett. **112**, 219 (2013).
[114] J. Shen, D. Zhang, J. Li, X. Li, Z. Sun, and S. Huang, Nano-Micro Lett. **5**, 281 (2013).
[115] M. S. Fan, J. H. Chen, C. T. Li, K. W. Cheng, and K. C. Ho, J. Mater. Chem. A **3**, 562 (2015).
[116] S. Wozny, K. Wang, and W. Zhou, J. Mater. Chem. A **1**, 15517 (2013).
[117] S. S. Mali, P. S. Patil, and C. K. Hong, ACS Appl. Mater. Interfaces **6**, 1688 (2014).
[118] S. Chen, H. Tao, Y. Shen, L. Zhu, X. Zeng, J. Tao, and T. Wang, RSC Adv. **5**, 6682 (2015).
[119] P. Dai, G. Zhang, Y. Chen, H. Jiang, Z. Feng, Z. Lin, and J. Zhan, Chem. Commun. **48**, 3006 (2012).
[120] J. Kong, Z.-J. Zhou, M. Li, W.-H. Zhou, S.-J. Yuan, R.-Y. Yao, Y. Zhao, and S.-X. Wu, Nanoscale Res. Lett. **8**, 464 (2013).
[121] H. Xie, Y. Sanchez, S. L. Marino, M. E. Rodríguez, M. Neuschitzer, D. Sylla, A. Fairbrother, V. I. Roca, A. P. Rodríguez, and E. Saucedo, ACS Appl. Mater. Interfaces **6**, 12744 (2014).
[122] J. Xu, X. Yang, Q. D. Yang, T. L. Wong, and C.-S. Lee, J. Phys. Chem. C **116**, 19718 (2012).
[123] S. K. Swami, N. Chaturvedi, A. Kumar, N. Chander, V. Dutta, K. Kumar, A. Ivaturi, S. Senthilarasu, and H. M. Upadhayay, Phys. Chem. Chem. Phys. **16**, 23993 (2014).
[124] H. Chen, D. Kou, Z. Chang, W. Zhou, Z. Zhou, and S. Wu, ACS Appl. Mater. Interfaces **6**, 20664 (2014).
[125] H. J. Kim, S. W. Kim, C. V. V. M. Gopi, S. K. Kim, S. S. Rao, and M. S. Jeong, J. Power Sources **268**, 163 (2014).
[126] W. Wang, X. Pan, W. Liu, B. Zhang, H. Chen, X. Fang, J. Yao, and S. Dai, Chem. Commun. **50**, 2618 (2014).
[127] K. Timmo, M. Altosaar, J. Raudoja, K. Muska, M. Pilvet, M. Kauk, T. Varema, M. Danilson, O. Volobujeva, and E. Mellikov, Solar Energy Mater. Solar Cells **94**, 1889 (2010).
[128] J. Briscoe and S. Dunn, Adv. Mater. **28** (2016).
[129] D. D. Kirubakaran, S. Pitchaimuthu, C. Ravi Dhas, P. Selvaraj, S. Z. Karazhanov, and S. Sundaram, Mater. Lett. **220**, 122 (2018).
[130] Y. Xie, C. Zhang, F. Yue, Y. Zhang, Y. Shic, and T. Ma, RSC Adv. **3**, 23264 (2013).
[131] J. Tao, J. Liu, J. He, K. Zhang, J. Jiang, L. Sun, P. Yang, and J. Chu, RSC Adv. **4**, 23977 (2014).
[132] B. Ananthoju, J. Mohapatra, M. K. Jangid, D. Bahadur, N. V. Medhekar, and A. Aslam, Sci. Rep. **6**, 35369 (2016).
[133] S.-L. Chen, J. Tao, H.-J. Tao, Y.-Z. Shen, A.-C. Xu, F.-X. Cao, J.-J. Jiang, T. Wanga, and L. Pan, Dalton Trans. **45**, 4513 (2016).
[134] Z.-Y. Xiao, Y.-F. Li, B. Yao, Z.-H. Ding, R. Deng, H.-F. Zhao, L.-G. Zhang, and Z.-Z. Zhang, RSC Adv. **5**, 103451 (2015).
[135] C. Coughlan and K. M. Ryan, Crys. Eng. Comm. **17**, 6914 (2015).
[136] X. Zhang, X. Wu, A. Centeno, M. P. Ryan, N. M. Alford, D. J. Riley, and F. Xie, Sci. Rep. **6**, 23364 (2016).
[137] M. Miyauchi, T. Hanayama, D. Atarashi, and E. Saka, J. Phys. Chem. C **116**, 23945 (2012).
[138] C. Mu, Y. Song, A. Liu, X. Wang, J. Hu, H. Ji, and H. Zhang, RSC Adv. **5**, 15749 (2015).
[139] H. Qing, Y. Zhu, Y. Hu, W. Hu, W. Zhou, J. Yi, and T. Shen, Mater. Lett. **176**, 177 (2016).
[140] H. Chen, Q. Ye, X. He, J. Ding, Y. Zhang, J. Han, J. Liu, C. Liao, J. Mei, and W. Lau, Green Chem. **16**, 3841 (2014).
[141] Q. Guo, H. W. Hillhouse, and R. Agrawal, J. Am. Chem. Soc. **131**, 11672 (2009).
[142] S. K. Swami, A. Kumar, and V. Dutta, Energy Proc. **33**, 198 (2013).
[143] M. P. Suryawanshia *et al.*, Electrochim. Acta **150**, 136 (2014).
[144] N. M. Shinde, D. P. Dubal, D. S. Dhawale, C. D. Lokhande, J. H. Kim, and J. H. Moon, Mater. Res. Bull. **47**, 302 (2012).
[145] Z. Li, J. C. W. Ho, K. K. Lee, X. Zeng, T. Zhang, L. H. Wong, and Y. M. Lam, RSC Adv. **4**, 26888 (2014).